Journal of
Composites Science

MDPI

Article

Influence of Timber-to-Concrete Connection Types on the Behaviour of Timber–Concrete Composite Structures

Dmitrijs Serdjuks *, Agris Rogainis, Elza Briuka, Janis Sliseris, Leonids Pakrastins and Vjaceslavs Lapkovskis *

Institute of Civil Engineering, Faculty of Civil and Mechanical Engineering, Riga Technical University, 6A Kipsalas Str., LV-1048 Riga, Latvia; agris.rogainis@hotmail.lv (A.R.); elza.briuka@rtu.lv (E.B.); janis.sliseris@rtu.lv (J.S.); leonids.pakrastins@rtu.lv (L.P.)
* Correspondence: dmitrijs.serdjuks@rtu.lv (D.S.); vjaceslavs.lapkovskis@rtu.lv (V.L.)

Abstract

The current study investigates the influence of timber-to-concrete connection types on the behaviour of timber–concrete composite (TCC) structures employing metal web timber joists. Two groups of laboratory specimens were prepared, each comprising four samples with push-joisted beams joined by oriented strand board (OSB) and cast with a concrete layer. One group utilised compliant timber-to-concrete connections via perforated steel tape angles, while the other employed rigid connections through epoxy adhesive and granite chips. The specimens, consisting of two 1390 mm long beams of grade PS10 timber, were tested under three-point bending. Experimental results and finite element analyses demonstrated that specimens with compliant connections exhibited 14–16% greater maximum vertical displacements but only a marginal 1.79% reduction in load-carrying capacity compared to those with rigid connections. Findings indicate that connection compliance markedly affects stiffness and deflection but has a minor impact on ultimate strength. These insights can guide optimisation of TCC members with metal web joists, balancing structural performance and design requirements in sustainable timber construction.

Keywords: timber-concrete composite (TCC); metal web timber joists; timber-to-concrete connections; rigid adhesive connection; perforated steel tape angles; structural optimisation; sustainable timber construction; push-joisted beams; shear connector

Academic Editor: Jiunn Jer Hwang

Received: 30 August 2025
Revised: 28 September 2025
Accepted: 2 October 2025
Published: 2 November 2025

Citation: Serdjuks, D.; Rogainis, A.; Briuka, E.; Sliseris, J.; Pakrastins, L.; Lapkovskis, V. Influence of Timber-to-Concrete Connection Types on the Behaviour of Timber–Concrete Composite Structures. *J. Compos. Sci.* **2025**, *9*, 593. https://doi.org/10.3390/jcs9110593

1. Introduction

The effectiveness of timber-concrete composite (TCC) structures depends on several factors, of which the most significant are the mechanical properties of the structural materials, the types of structural cross-sections utilised, the types of timber-to-concrete connections, and the mechanical properties of fasteners. Increasing effectiveness involves reducing the overall structural weight, enhancing stiffness and load-bearing capacity, and improving the aesthetic parameters of buildings [1–5]. TCC structures are widely employed as roof and floor structures in multi-storey timber buildings. The type of timber-to-concrete connection and the selected fasteners play a crucial role in transferring internal forces within the cross-section between the concrete and timber layers [6]. Timber-to-concrete connections can be categorised as rigid, semi-rigid, and compliant. Each of these types offers specific advantages and disadvantages concerning effectiveness. Inflexible and compliant timber-to-concrete connections are the two main contrasting cases, with the former

providing increased material effectiveness and the latter offering ductility in the timber-to-concrete connection. Both behaviours are desirable for TCC, but they often conflict, and having both simultaneously can be problematic. Rigid timber-to-concrete connections can be realised using adhesive bonds, such as the granular chips method [6].

Grooved connections, different types of metal fasteners, and glued-in steel connections can realise compliant timber-to-concrete connections [1,7–9]. Perforated steel details, glued into the timber layer or joined with it using screws and nails, are also utilised in compliant timber-to-concrete connections. The optimal combination of stiffness and compliance for timber-to-concrete connections in TCC requires behavioural investigations of both rigid and compliant types of connections. Adding perforated steel tape as a shear connector to the adhesive timber-to-concrete joint allows the creation of a hybrid timber-concrete composite structural member with increased stiffness and reliability [10,11]. Additionally, the perforated steel plate connection in TCC is more effective than notched timber with screws when tested for fire safety, resulting in less deflection at higher temperatures and a slower decrease in the connectors' slip modulus [8].

In the event of adhesive connection failure, the perforated steel tape can prevent the disintegration of the structural member and enable the timber and concrete layers to bear the applied loads. The perforated steel element and the granite chip connection could enhance fire safety and mitigate brittle collapse in adhesively bonded TCC structures. However, predicting the behaviour of combined adhesive and mechanical timber-to-concrete connections—such as those realised by the granite chips method in conjunction with the mechanical fasteners provided by perforated steel tape—requires detailed information on each type of connection separately. Information on the behaviour of TCC with adhesive timber-to-concrete connections and the combination of adhesive and mechanical connections implemented using perforated steel tape is available in various sources [11–13]. The comparative behaviour of rigid and compliant timber-to-concrete connections, the discussion on damage control, and post-damage reparability has been comprehensively outlined by He et al. [14].

In the current work, particular focus has been placed on the separate investigation of the compliant timber-to-concrete connection provided by perforated steel tape, used as a shear connector. The results of this investigation should be compared with those obtained from similar specimens with adhesive timber-to-concrete connections, realised by the granite chips method (Figure 1).

Figure 1. The adhesive granite chips method prepares timber members for connection with the concrete layer.

The effectiveness of the structural materials can be enhanced by selecting more optimised types of cross-sections for the structural members [15–18]. Combining timber–concrete composite structures with push-joisted beams further improves the benefits, increasing the stiffness of floor and roof structures [19–21]. A simplified design method and finite element modelling (FEM) will be utilised to predict the behaviour of the TCC structure with push-joisted beams analytically. The behaviour of the TCC structure with a push-joisted beam, featuring a rigid adhesive and compliant timber-to-concrete connection provided by perforated steel tape used as a shear connector, should be investigated and compared analytically and through laboratory experiments. The load-carrying capacity of the structures should also be examined. Therefore, the objective of the current investigation is to compare the behaviours.

2. Materials and Methods

2.1. General Approach

The behaviour of the TCC structure with push-joisted beams, featuring a rigid adhesive and a compliant timber-to-concrete connection provided by perforated steel tape used as a shear connector, was investigated analytically using the simplified design method, finite element modelling (FEM), and laboratory experiments. The simplified design method enables the determination of the maximum regular and shear stresses acting in the concrete and OSB layers and in the chords of the push-beams. The maximum vertical displacements of the TCC specimens can also be estimated by considering the influence of bending moments and shear forces. The simplified design method is explained in detail in the source [15], based on the transformed section method and the γ-method described in Annexe B of EN 1995-1-1 [19] for mechanically jointed beams [21]. This method was successfully validated for the TCC structure with a push-joisted beam featuring a rigid adhesive timber-to-concrete connection, realised by the granite chips method [21]. The current study was conducted to validate the technique for a compliant timber-to-concrete connection provided by perforated steel tape. The three-point bending test involved four laboratory TCC specimens with a compliant timber-to-concrete connection, detailed in Section 2.2. The results were compared with the analogous results for identical specimens with a rigid adhesive timber-to-concrete connection, which was realised using the granite chips method. The behaviour of the specimens with the compliant timber-to-concrete connection was predicted using the FE method, implemented with Ansys R2 2022 software. The FE model is described in detail in Section 2.3.

2.2. Laboratory Experiment

A group of four laboratory specimens with push-joisted beams and a compliant timber-to-concrete connection provided by perforated steel tape angles was prepared. The specimens include two push-joisted beams. Each beam has a length of 1390 mm. The two beams are joined by an oriented strand board (OSB/3) (Kronospan Ltd., Wrexham, Latvia), measuring 400 mm in width and 18 mm in thickness. The depth of the beams' cross-sections is 253 mm. These geometrical parameters correspond to beams of grade PS10. The top and bottom chords of the beams have identical cross-sections made from solid timber, measuring 95 mm $\times$ 65 mm. Steel lattice members connect the chords with a 47 $\times$ 1mm C-type cross-section. Timber struts have 95 $\times$ 95 mm cross-sections, made from solid timber. Three bracing members with 100 mm $\times$ 45 mm cross-sections connect the bottom chords of the beams. A concrete layer, 50 mm thick, was applied using the self-levelling mass SakretBAM, produced by SAKRET (Riga, Latvia). The main mechanical properties of the materials used are shown in Table 1.

Table 1. Mechanical properties of materials used in experiments.

Material	Property	Value
Concrete C20/25	Compressive strength, f_c, MPa Tensile strength, f_t, MPa Elastic modulus, E_c, MPa	25 2.2 27,000
Timber PS10	Tensile strength, f_t, MPa Compressive strength, f_c, MPa Elastic modulus, E_t, MPa	15–20 20–25 11,000
Steel S275	Yield strength, f_y, MPa Ultimate tensile strength, f_u, MPa Elastic modulus, E_s, MPa	275 360–510 210,000
Polypropylene fibres	Tensile strength, MPa	300–450

Perforated steel angles, 2 × 50 × 60 × 160 mm, provide the compliant timber-to-concrete connection (Figure 2a,b). The source recommends configuring the structural member and timber-to-concrete connection [19,21]. The mould filling with SakretBAM is shown in Figure 3a.

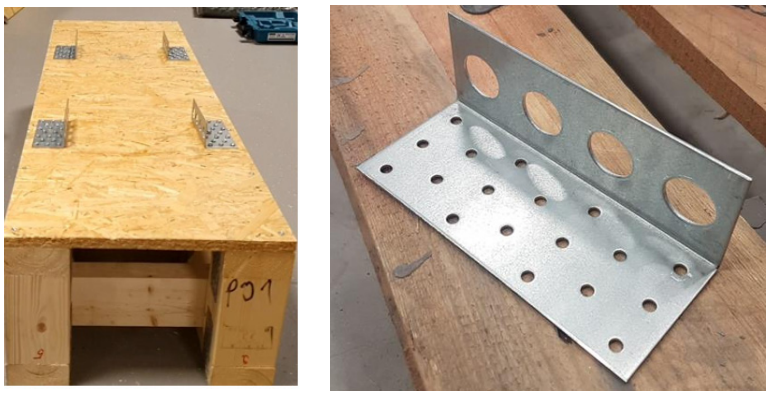

(**a**) (**b**)

Figure 2. Providing the compliant timber-to-concrete connection with the perforated steel angles: (**a**) placement of the angles on the OSB/3 surface; (**b**) perforated steel angle 2 × 50 × 60 × 160 mm.

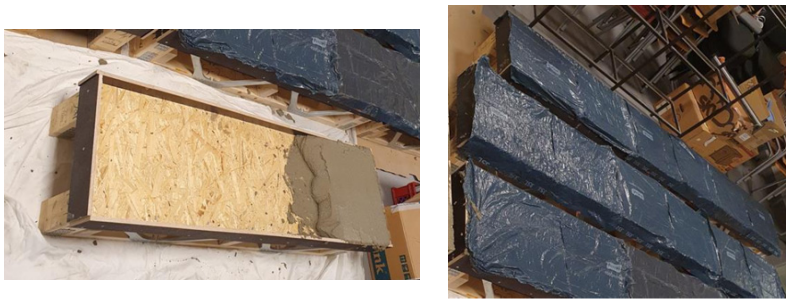

(**a**) (**b**)

Figure 3. Process of the laboratory specimens preparation: (**a**) The mould filling by the self-levelling mass SakretBAM; (**b**) The surface of the self-levelling mass SakretBAM covered by the polyethelene foil.

The polyethene foil covered the surface of the self-levelling mass SakretBAM to prevent the development of initial cracks on the concrete surface (Figure 2b). The specimens were cured over 28 days to allow the concrete layer to reach its design strength and for the specimens to achieve their specified load-carrying capacity [21].

The specimens were loaded using the testing device CONTROL model 50-C/1400* up to their load-carrying capacity of 24 kN, as evaluated by the simplified design method described above. The specimens were loaded according to a three-point bending scheme, with the concentrated force applied at the centre of the span, which measures 1390 mm. The specimens were loaded twice up to 24 kN, and then the load was removed. The third loading continued until the specimens collapsed. The actual load-carrying capacities of the specimens and the relationships between load and the maximum vertical displacements in the middle of the span were determined during the laboratory experiment.

2.3. Finite Element Modelling

The finite element model was developed using ANSYS R2 2022 software to analyse timber-concrete composite specimens with two distinct connection types: compliant connections using perforated steel tape angles and rigid adhesive connections through the granite chips method.

The FEM model employed a sophisticated multi-element approach tailored to the specific characteristics of each structural component:

- Beam Elements: Beam 188 elements were utilised for modelling the top and bottom chords of the push-joisted beams as well as the bracing members. This element type is particularly suitable for linear structural components where bending behaviour dominates.
- Shell Elements: Shell finite elements were employed for modelling the concrete layer, OSB3 plate, steel lattice members, and perforated steel angles. This approach allows for an accurate representation of thin-walled components while maintaining computational efficiency.
- Solid Elements: SOLID-FE were specifically implemented for the concrete layer to enable crack development simulation, providing detailed insight into failure mechanisms.

The model incorporated realistic material properties based on standard specifications and experimental characterisation:

- Concrete C20/25: Compressive strength of 25 MPa, tensile strength of 2.2 MPa, and elastic modulus of 27,000 MPa.
- Timber (C24 for FEM, PS10 for experiments): Tensile strength of 15–20 MPa, compressive strength of 20–25 MPa, and elastic modulus of 11,000 MPa.
- Steel S275: Yield strength of 275 MPa, ultimate tensile strength of 360–510 MPa, and elastic modulus of 210,000 MPa.

The specimens consisted of two 1390 mm long push-joisted beams joined by an 18 mm thick OSB3 board measuring 400 mm in width. The beam cross-sections had a depth of 253 mm, corresponding to PS10 grade specifications. Top and bottom chords featured identical 95 × 65 mm cross-sections, while steel lattice members utilised 47 × 1 mm C-type profiles. A 50 mm-thick concrete layer was applied using self-levelling mass.

The shell finite element type was utilised to model the concrete layer, OSB/3 plate, and steel lattice members. The SOLID-FE was also used to model the concrete layer to simulate crack development. The concrete layer's strength class was assumed to be C20/25. The solid timber with a C24 strength class was considered for the top and bottom chords, struts, and bracing members. The steel used for the lattice members was of S275 strength class. The simplified stress–strain curve for S275 steel, incorporated into the FE modelling, is shown in Figure 4.

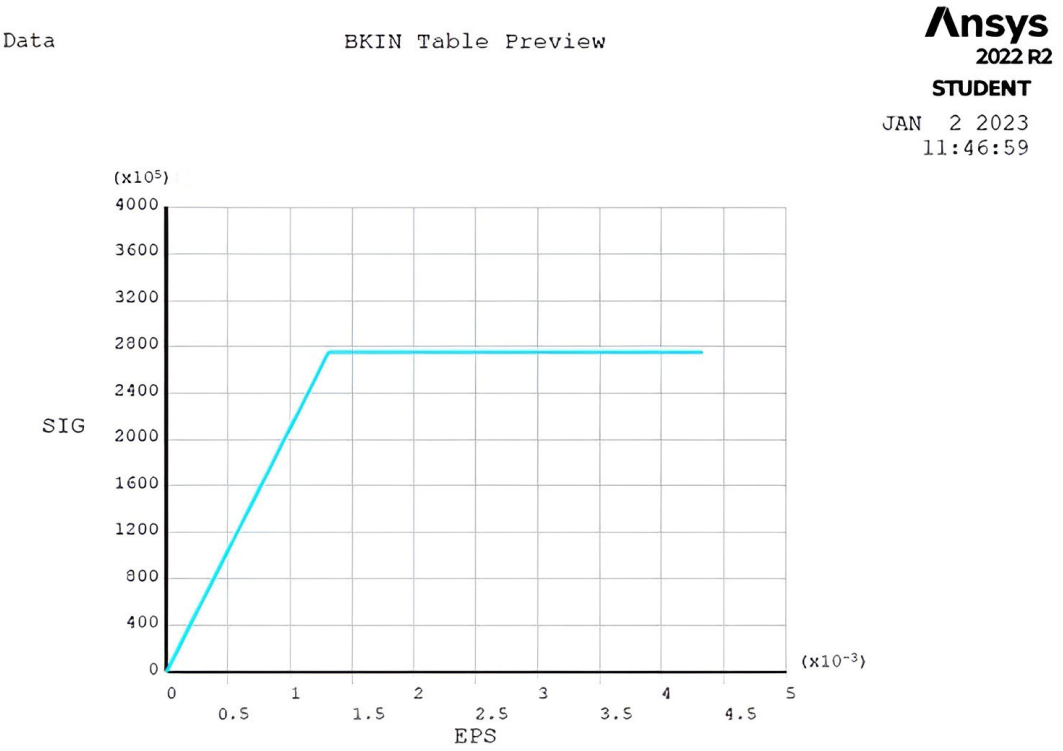

Figure 4. Simplified stress–strain curve for the S275 strength class steel.

The steel members—lattice elements and perforated steel angles, modelled using the shell finite element type—are shown in Figure 5a. The connection of the lattice member with the specimen's bottom chord is illustrated in Figure 5b.

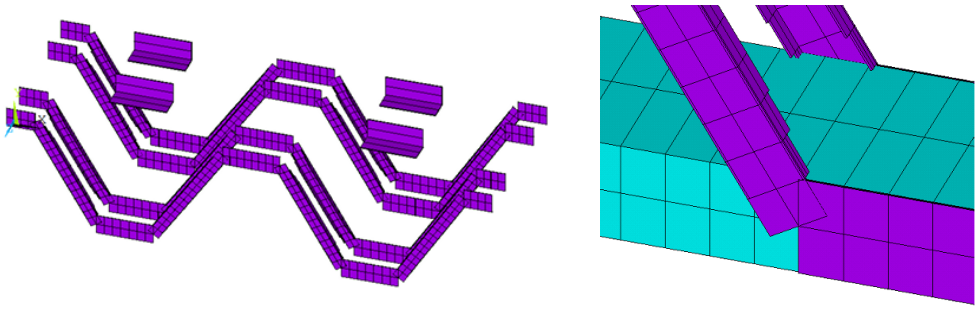

(**a**) (**b**)

Figure 5. Modelling of the steel details of the specimens by the software Ansys R2 2022: (**a**) elements of the lattice and perforated steel angles, modelled by the shell finite element type; (**b**) connection of the lattice member with the bottom chord of the specimen [21].

The connection between the top chord, lattice members, OSB/3, and concrete layers is shown in Figure 5. The concrete and OSB/3 layers, modelled using shell-type finite elements, are indicated by red and green colours, respectively. The top chord, shown in Figure 6, and the bottom chord, shown in Figure 5b, are modelled with Beam 188 finite elements and are displayed in the figures in blue colour.

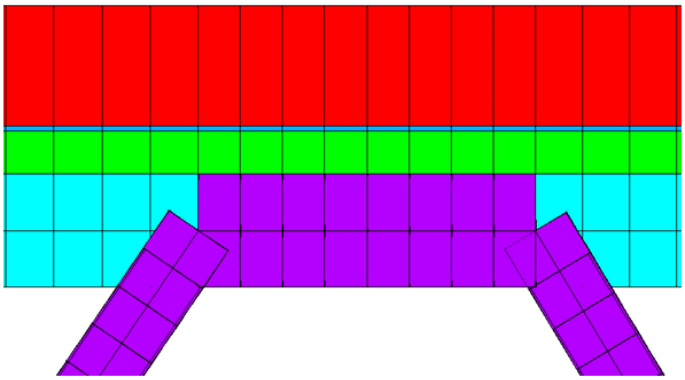

Figure 6. Connection of the top chord with the lattice members and with the OSB/3 and concrete layers.

The analogous FE model, but with the adhesive timber-to-concrete connection, is described in [15]. The results obtained for the models with a compliant timber-to-concrete connection provided by perforated steel tape angles and an adhesive timber-to-concrete connection realised by the granite chips method are compared and discussed in the next chapter of the present study.

3. Results and Discussions

3.1. Results of Laboratory Experiments and Finite Element Modelling

A group of four laboratory specimens with push-joisted beams and a compliant timber-to-concrete connection provided by perforated steel tape angles were investigated through laboratory experiments, the simplified design method, and FEM analysis. As mentioned, the specimens were tested using a three-point bending scheme, as shown in Figure 7.

Figure 7. Testing of the specimens in laboratory conditions.

The specimens were supported on square steel profiles measuring 100 × 100 × 5 mm. The distance between the centres of the supports was 1390 mm. Two digital deflectometers positioned at the mid-span of the specimens measured the maximum vertical displacements (Figure 8).

Figure 8. Testing setup with sensors placed 4 cm away from the centre of gravity of the element.

The relationship between the maximum vertical displacements and the applied load is shown in Figure 9 for all four specimens. The actual load-carrying capacities of all the specimens were determined. The most significant maximum vertical displacement, measuring 16.29 mm, was observed in specimen S-4-3. The smallest maximum vertical displacement, at 14.72 mm, was recorded for specimen S-4-2. The first number in the specimen designations indicates the group number, while the second specifies the individual specimen within that group. The specimens under consideration belong to group 4. The previous study described the first three groups of specimens and their testing results [15].

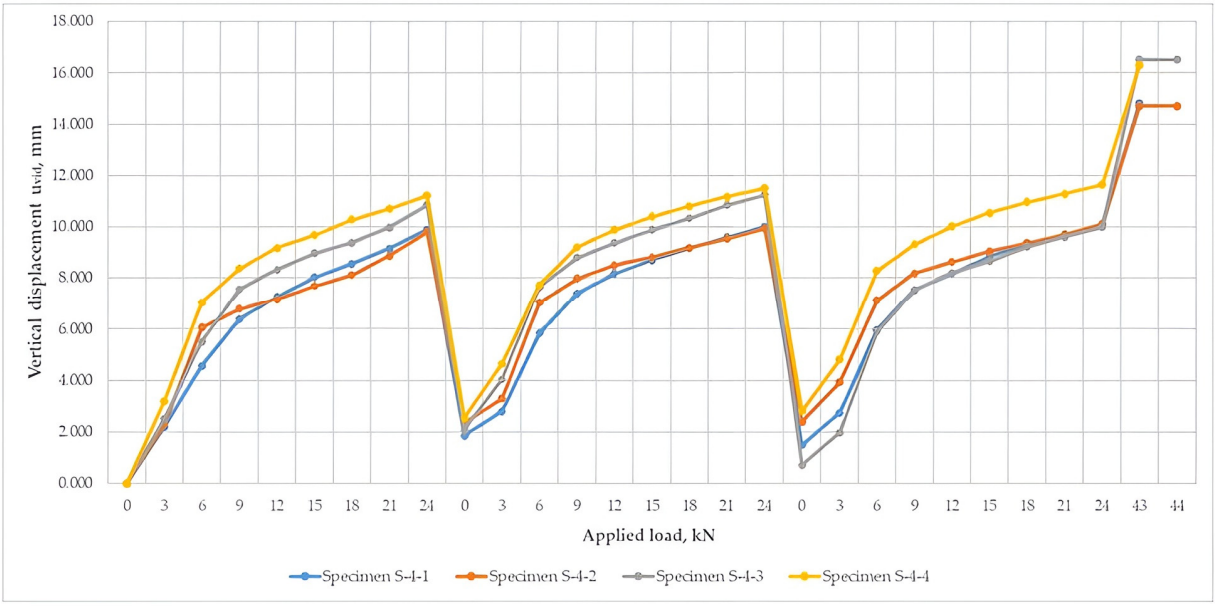

Figure 9. Dependence of the maximum vertical displacements on the vertical load, applied as a concentrated force in the middle of the span, for four laboratory specimens for three stages of loading.

The load-carrying capacities of the specimens are 43.27, 44.89, 44.82, and 43.39 kN for specimens S-4-1, S-4-2, S-4-3, and S-4-4, respectively (Figure 10a). Thus, the maximum load-carrying capacity observed was 44.89 kN for specimen S-4-2. The difference between the specimens' maximum and minimum load capacities did not exceed 3.74%. However, the average load-carrying capacity of the specimens, calculated as 43.99 kN, exceeds the load capacity obtained via the simplified design method described above by 83.30%.

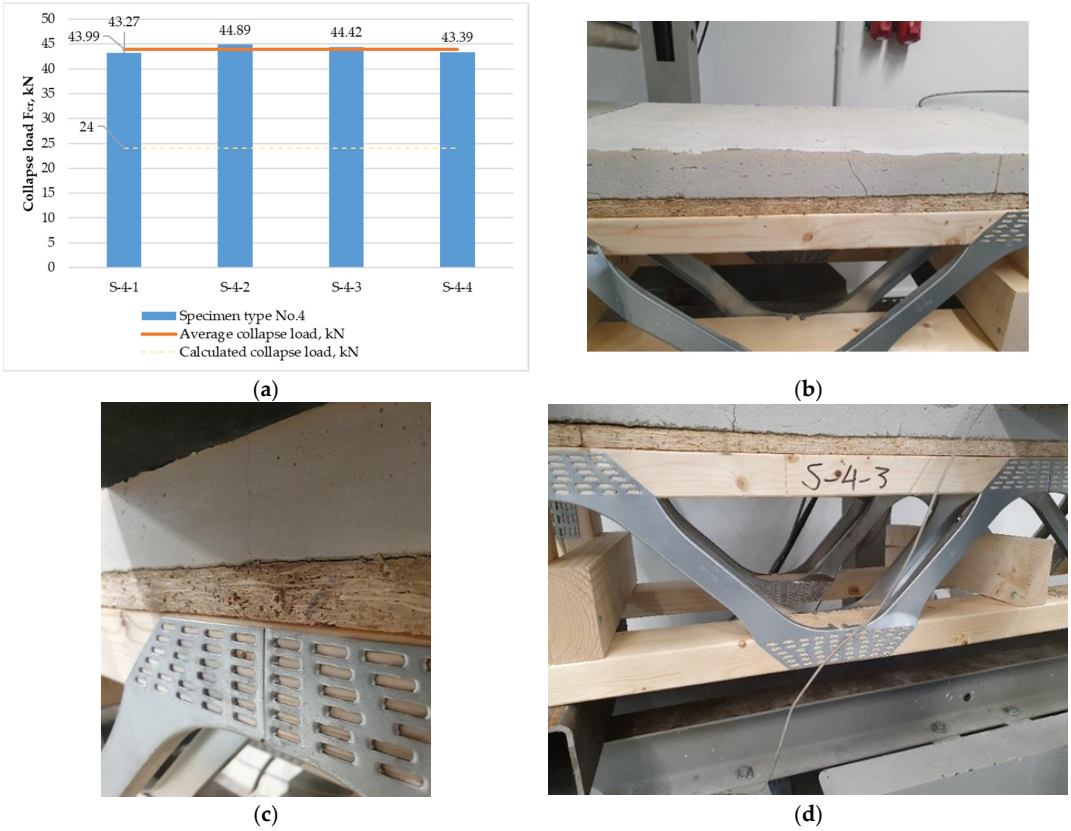

Figure 10. Load-carrying capacities of the laboratory specimens: (**a**) and its failure mode: cracks development in the concrete layer in the zone of the specimens support; (**b**,**c**) cracks development in the concrete layer in the middle of the span; (**d**) buckling of the compressed member of the lattice.

Figure 10b–d illustrate the failure modes of the laboratory specimens. Buckling of the compressed web member occurs alongside the development of cracks in the concrete layer, particularly in the zone where the perforated steel angles are installed and in the middle of the specimens' span. The cracks develop in a direction perpendicular to the longitudinal axis of the specimens precisely at the moment of failure. These cracks emerge in the zones where the perforated angles are placed. The stress concentrations in these zones may be the cause of crack development. During specimen failure, the progression of cracks leads to partial disintegration. This disintegration can be mitigated by adding polyethene or other fibres to the concrete mixture [15].

The failure mode observed in the laboratory specimens indicates that the structural materials are not being utilised to their full potential. The preferable failure mode would be the simultaneous failure of the bottom chord of the push-beam and the lattice. Therefore, strengthening the lattice of the push-beams—either by using steel profiles with greater load-carrying capacity in compression or by adding additional lattice members—could be considered as potential ways to enhance the load-carrying capacity of these TCC members. An area of particular interest is using composite profiles as timber-to-concrete fasteners instead of steel to minimise stress concentrations in the zones where fasteners are installed.

The generalised relationships of the maximum vertical displacements versus the vertical load, obtained using the simplified design method, laboratory experiment (mean value over all three loadings), and FE method with the concrete layer modelled by shell and solid finite element types for the rigid and compliant timber-to-concrete connections, are shown in Figure 11. Compared to the results obtained from the FE model with the compliant timber-to-concrete connection, the maximum vertical displacements predicted by the simplified design method show an average difference of 24.7%. The smallest difference of 1.2% was observed at a load of 3 kN. The most significant difference, 37.30%, occurred at a load of 12 kN. During the FE modelling, the rigid timber-to-concrete connection resulted in a larger deviation from the laboratory results than the compliant one. Therefore, in FE modelling of structural members with push-joisted beams and a compliant timber-to-concrete connection provided by perforated steel tape angles, the connection's compliance should be considered, as it significantly influences the laboratory specimens' behaviour.

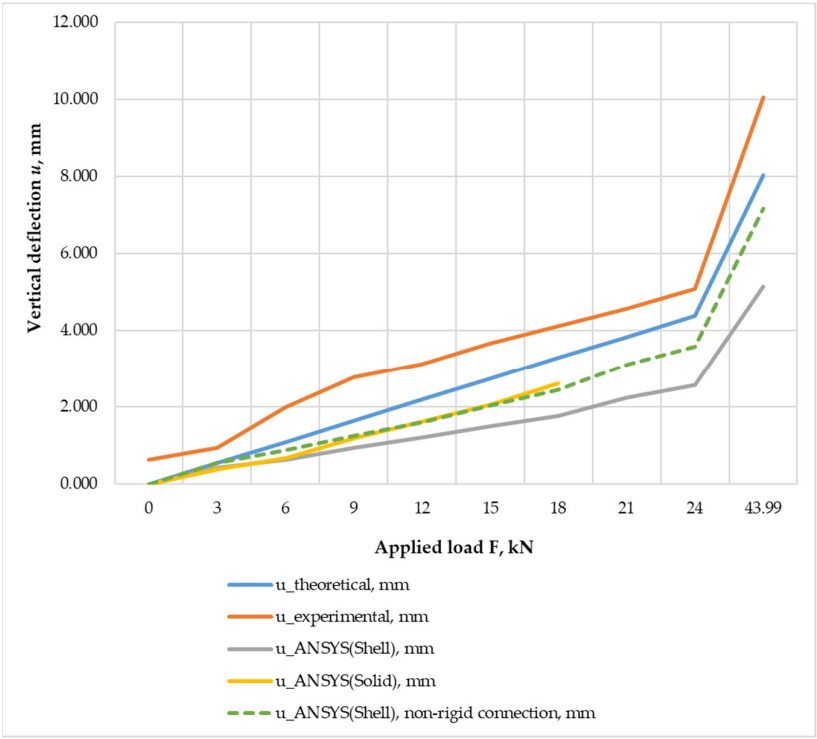

Figure 11. Generalised dependence of the maximum vertical displacements on the vertical load, obtained by the simplified design method, laboratory experiment (mean value for all three loadings) and FE method with the concrete layer modelled by the SHELL and SOLID finite element types for the rigid and compliant timber-to-concrete connections.

The values of the normal stresses, determined by the simplified design method in the concrete layer of the laboratory specimens with a compliant timber-to-concrete connection provided by perforated steel tape angles, vary from 0.92 to 7.35 MPa as the load increases from 3 to 24 kN, respectively. The same normal stresses, calculated using the FE method with the concrete layer modelled by shell and solid finite element types, range from 0.93 to 7.65 MPa and 1.60 to 8.16 MPa, respectively. The difference between the normal stresses determined by the simplified design method and those obtained via the FE method with the concrete layer modelled by shell and solid finite elements varies from 1.20 to 4.00% and 47.90 to 74.00%, respectively. Based on the results obtained in the study [21], both from laboratory experiments and FE analysis, it can be concluded that the considered simplified design method is suitable for predicting the behaviour of TCC structural members with

push-joisted beams and a compliant timber-to-concrete connection provided by perforated steel tape angles.

3.2. Comparison of the Results Obtained for the Specimens with Compliant and Adhesive Timber-to-Concrete Connections

The behaviour of the TCC structural members with push-joisted beams, featuring a rigid adhesive and compliant timber-to-concrete connection provided by perforated steel angles used as a shear connector, should be compared, as previously mentioned. The maximum vertical displacements, recorded for the groups of specimens with rigid adhesive and compliant timber-to-concrete connections, as functions of the applied loads, are shown in Figure 12. The results obtained for the specimens with compliant timber-to-concrete connections—via laboratory experiment, simplified design method, and FE method with the concrete layer modelled by shell and solid finite element types—are described above in Section 3.1. Similar results, obtained for the specimens with rigid timber-to-concrete connections, have been previously documented and are described in detail in the work of [21].

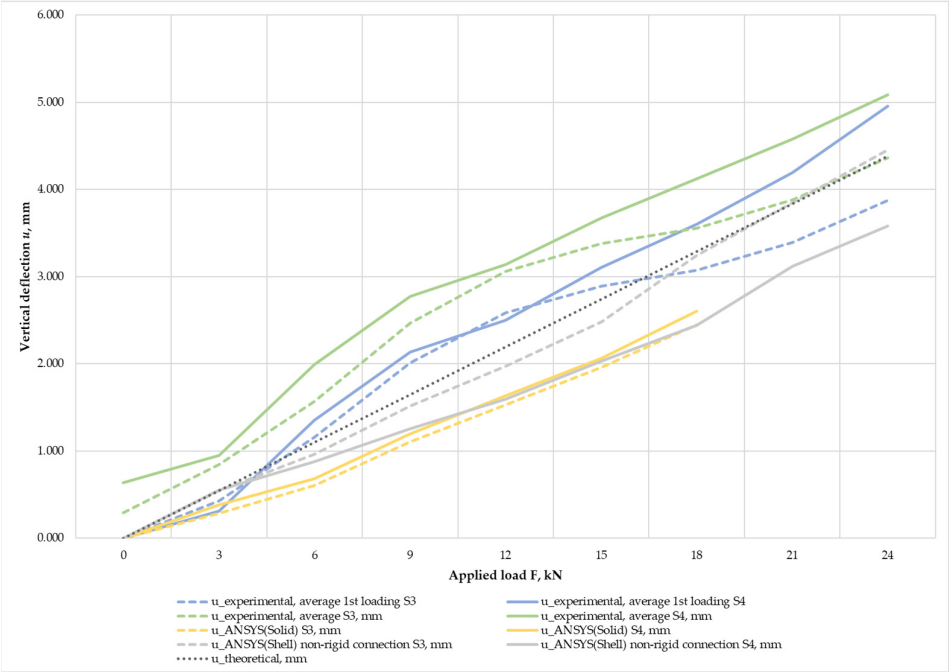

Figure 12. Generalised dependence of the maximum vertical displacements on the vertical load, obtained by the simplified design method, laboratory experiment (mean value for all three loadings) and FE method with the concrete layer modelled by the SHELL and SOLID finite element types for the groups of specimens with the rigid adhesive and compliant timber-to-concrete connections.

Comparison of the maximum vertical displacements obtained by the laboratory experiment for both considered groups of specimens indicates that the rigid adhesive timber-to-concrete connection reduces the mean vertical displacements by 14–16% compared to specimens where perforated steel angles provide a compliant connection.

The mean value of the load-carrying capacity for the specimens with the rigid adhesive timber-to-concrete connection increases by only 1.79% compared to the compliant connection. The average load-carrying capacity for the group with rigid and compliant connections is 45.81 kN and 44.99 kN, respectively. Therefore, it can be concluded that the compliance of the timber-to-concrete connections affects the behaviour of the specimens,

with the specimens using metal-web timber joists being less efficient than those with solid timber bases.

The finite element analysis revealed several critical failure mechanisms that govern the structural behaviour of timber-concrete composite members. The most significant failure mode observed was buckling of the steel lattice web members under compression loading. This premature failure prevented the structural materials from reaching their full potential capacity. Progressive crack formation occurred in the concrete layer, particularly concentrated in two critical zones: near the perforated steel angles and at the mid-span of the specimens. These cracks developed perpendicular to the longitudinal axis precisely at the moment of structural failure. The zones where perforated steel angles were installed experienced significant stress concentrations, which became the primary catalyst for crack initiation and propagation. During specimen failure, the progression of cracks led to partial disintegration of the concrete layer. The research noted that this disintegration could be mitigated through the addition of polypropylene or other fibres to the concrete mixture.

The observed failure patterns indicated that the structural materials were not being utilised to their full potential. The preferable failure mode would involve simultaneous failure of the bottom chord and lattice members, suggesting opportunities for structural optimisation through lattice strengthening or the use of composite profiles as timber-to-concrete fasteners.

The finite element model provided detailed stress distribution patterns and quantitative stress analysis across different structural components. The analysis revealed significant variations in normal stress patterns depending on the analysis method employed:

- Simplified Design Method: Normal stresses in the concrete layer ranged from 0.92 MPa at 3 kN loading to 7.35 MPa at 24 kN loading.
- Shell Element FEM: Stress values ranged from 0.93 MPa to 7.65 MPa for the same loading range, showing excellent correlation with the simplified method, with differences in only 1.2% to 4.0%.
- Solid Element FEM: Higher stress predictions ranging from 1.60 MPa to 8.16 MPa, with differences of 47.9% to 74.0% compared to the simplified method, indicating sensitivity to modelling approaches.

The comparison of the maximum normal stresses in the concrete layers—determined by the FE method with the concrete layer modelled using shell and solid finite element types—shows that higher normal stress values characterise specimens with compliant connections. The maximum normal stresses increased by 20% and 33% for the shell and solid finite element types, respectively. The stresses acting in the bottom chords of the specimens increased by 18% and 12% for the shell and solid finite element types, respectively.

3.3. Future Research Directions

The research demonstrates that connection compliance markedly affects structural stiffness and deflection while having minimal impact on ultimate strength. This finding has significant implications for design optimisation, where the choice between rigid adhesive and compliant connections can be guided by specific structural performance requirements.

The study identified several areas for potential structural enhancement, including lattice strengthening through higher-capacity steel profiles or additional lattice members, and the investigation of composite materials for timber-to-concrete fasteners to minimise stress concentrations. Future research directions include optimisation of geometric parameters, material properties, and perforation parameters of steel tape angles used as fasteners.

The general trends associated with the application of the compliant timber-to-concrete connection provided by perforated steel tape angles in TCC members with push-joisted beams were investigated in the current study. It was established that the compliance of

the timber-to-concrete connection mainly influences the maximum vertical displacements of the specimens, which are directly related to its stiffness. The load-carrying capacity decreases when the connection lacks compliance, although this reduction is insignificant. Further investigation into optimising structural members with push-joisted beams and a compliant timber-to-concrete connection, provided by perforated steel tape angles, is a probable direction for future research. Parameters such as total material consumption, load-carrying capacity, and stiffness could be optimised criteria. Factors such as the geometric parameters of the structural members, the mechanical properties of the materials, and the perforation parameters of the perforated steel tape angles used as fasteners should be considered as the primary factors for the optimisation task.

Possibility to avoid the members' disintegration in the course of its failure should be found. Adding the MAPEI PP-Fibre M6 polypropylene fibres to the concrete layer decreases the adhesive timber-to-concrete connection's brittleness and prevents specimens' disintegration during their collapse (Figure 13). The concrete layer did not collapse in the case (Figure 13b), but its mechanical properties and total specimens' stiffness decreased in this case.

(**a**) (**b**)

Figure 13. Failure modes of the TCC specimens without (**a**) and with (**b**) the fibres added to the concrete layer in the case of adhesive timber-to-concrete connection.

However, adding polypropylene fibres decreases the members' load-carrying capacity, increasing the maximum vertical displacements. So, investigating the fibre-concrete mechanical properties, which reduces the brittleness of the timber-to-concrete adhesive connection without decreasing the members' load-carrying capacity and stiffness, is one more probable direction for further investigations.

The potential use of perforated industrial waste materials for perforated steel tapes and angles in timber-to-concrete connections can also be explored, aligning with the goals of sustainable resource use and waste recycling from economic activities, which are two primary environmental objectives.

An additional investigation area involves using composite materials, such as fibre-reinforced plastics, for compliant timber-to-concrete connections. Structural materials with lower mechanical properties than steel can help prevent crack development in the compressed concrete layer of TCC members by reducing stress concentrations in the fastener zone.

4. Conclusions

The proposed study investigated the behaviour of timber–concrete composite (TCC) structures with push-joisted beams using two types of timber-to-concrete connections: compliant connections provided by perforated steel tape angles and rigid adhesive connections realised by the granite chips method. Laboratory experiments, finite element (FE) modelling, and a simplified analytical design method were employed to evaluate the specimens' maximum vertical displacements and load-carrying capacities. The main conclusions of the conducted research are as follows:

- Specimens with rigid adhesive timber-to-concrete connections showed a reduction in mean maximum vertical displacements by 14–16% compared to specimens with compliant connections using perforated steel tape angles. This indicates increased structural stiffness provided by the adhesive connection.
- The average load-carrying capacity increased marginally by approximately 1.79% for specimens with rigid adhesive connections relative to those with compliant connections, with average capacities of 45.81 kN and 44.99 kN, respectively.
- Normal stresses in the concrete layer of specimens with compliant connections ranged from 0.92 MPa to 7.35 MPa as the applied load increased from 3 kN to 24 kN (simplified design method), and corresponded closely with FE model predictions using shell finite elements (0.93–7.65 MPa). The FE model with solid elements predicted higher stresses, indicating sensitivity to modelling approaches.
- The simplified design method based on the transformed section method and γ-method was validated as effective for predicting the behaviour of TCC members with compliant timber-to-concrete connections, facilitating simplified yet reliable design procedures.
- The choice between rigid adhesive and compliant connections can be guided by structural performance requirements—adhesive connections provide higher stiffness (lower deflections). In contrast, compliant connections offer comparable strength with potentially improved ductility and material sustainability benefits.

Author Contributions: Conceptualization, D.S., A.R. and E.B.; methodology, D.S., A.R. and E.B.; software, J.S.; validation, A.R., D.S. and E.B.; formal analysis, J.S.; investigation, A.R.; resources, E.B.; data curation, J.S.; writing—original draft preparation, D.S., V.L., J.S. and L.P.; writing—review and editing, V.L.; visualisation, A.R., E.B. and J.S.; supervision, D.S., E.B. and L.P.; project administration, D.S. and V.L. All authors have read and agreed to the published version of the manuscript.

Funding: This research was funded by a Doctoral academic career grant No. 1067. European Union Recovery and Resilience Facility funded project No. 5.2.1.1.i.0/2/24/I/CFLA/003 "Consolidation and management changes at Riga Technical University, Liepaja University, Rezekne Academy of Technologies and the Latvian Maritime Academy and Liepaja Maritime College towards excellence in higher education, science and innovation.

Data Availability Statement: The data presented in this study are available on request from the corresponding author due to research of commercialisaton of final products.

Conflicts of Interest: The authors declare no conflicts of interest.

References

1. Estévez-Cimadevila, J.; Martín-Gutiérrez, E.; Suárez-Riestra, F.; Otero-Chans, D.; Vázquez-Rodríguez, J.A. Timber-Concrete Composite Structural Flooring System. *J. Build. Eng.* **2022**, *49*, 104078. [CrossRef]
2. Vijayakumar, R.; Pannirselvam, N. Behaviour of a New Type of Shear Connector for Steel-Concrete Composite Construction. *Mater. Today Proc.* **2021**, *40*, S154–S160. [CrossRef]
3. Al-Zaidee, S.R.; Al-Hasany, E.G. Finite Element Modeling and Parametric Study on Floor Steel Beam Concrete Slab System in Non-Composite Action. *J. Eng.* **2018**, *24*, 95–113. [CrossRef]
4. Premrov, M.; Žegarac Leskovar, V. Innovative Structural Systems for Timber Buildings: A Comprehensive Review of Contemporary Solutions. *Buildings* **2023**, *13*, 1820. [CrossRef]
5. Liu, T.; Chen, L.; Yang, M.; Sandanayake, M.; Miao, P.; Shi, Y.; Yap, P.-S. Sustainability Considerations of Green Buildings: A Detailed Overview on Current Advancements and Future Considerations. *Sustainability* **2022**, *14*, 14393. [CrossRef]
6. Buka-Vaivade, K.; Serdjuks, D. Behavior of Timber-Concrete Composite with Defects in Adhesive Connection. *Procedia Struct. Integr.* **2022**, *37*, 563–569. [CrossRef]
7. Dias, A.; Skinner, J.; Crews, K.; Tannert, T. Timber-Concrete-Composites Increasing the Use of Timber in Construction. *Eur. J. Wood Prod.* **2016**, *74*, 443–451. [CrossRef]
8. Andaque, H.; Sadeghi, K. Comparison Between Timber Concrete Composite Slab and Solid Slab for Residential Buildings. *IJISRT* **2023**, *8*, 612–623.

9. Buka-Vaivade, K.; Serdjuks, D.; Pakrastins, L. Cost Factor Analysis for Timber–Concrete Composite with a Lightweight Plywood Rib Floor Panel. *Buildings* **2022**, *12*, 761. [CrossRef]
10. Mironovs, V.; Kuzmina, J.; Serdjuks, D.; Usherenko, Y.; Lisicins, M. Sustainable Lifecycle of Perforated Metal Materials. *Materials* **2023**, *16*, 3012. [CrossRef] [PubMed]
11. Skincs, A.; Serdjuks, D.; Buka-Vaivade, K.; Goremikins, V.; Mohamed, A.Y. Steel and Composite Tapes in Timber to Concrete Joint. In *Sustainable Energy Systems: Innovative Perspectives*; Sinitsyn, A., Ed.; Lecture Notes in Civil Engineering; Springer International Publishing: Cham, Switzerland, 2021; pp. 68–79. ISBN 978-3-030-67654-4.
12. Mönch, S.; Campos, J.A.A.; Dias, A.M.P.G.; Kuhlmann, U. Influence of the Geometric Properties, the Timber–Concrete Interface, and the Load Protocol on the Mechanical Properties of Timber–Concrete Composite Connections. *Appl. Sci.* **2024**, *14*, 6768. [CrossRef]
13. He, X.; Yam, M.C.H.; Ke, K.; Zhou, X.; Zhang, H.; Gu, Z. Behaviour Insights on Damage-Control Composite Beam-to-Beam Connections with Replaceable Elements. *Steel Compos. Struct.* **2023**, *46*, 773–791. [CrossRef]
14. Briuka, E.; Serdjuks, D.; Akishin, P.; Sahmenko, G.; Podkoritovs, A.; Ozolins, R. Behaviour Analysis of Beam-Type Timber and Timber-Concrete Composite Panels. *Appl. Sci.* **2024**, *14*, 7403. [CrossRef]
15. Deam, B.L.; Fragiacomo, M.; Buchanan, A.H. Connections for Composite Concrete Slab and LVL Flooring Systems. *Mater Struct* **2008**, *41*, 495–507. [CrossRef]
16. Winandy, J.E.; Morrell, J.J. Improving the Utility, Performance, and Durability of Wood- and Bio-Based Composites. *Ann. For. Sci.* **2017**, *74*, 25. [CrossRef]
17. Jiang, B.; Zhang, J.; Ohsaki, M. Optimization of Branching Structures for Free-Form Surfaces Using Force Density Method. *J. Asian Archit. Build. Eng.* **2022**, *21*, 1458–1471. [CrossRef]
18. Zhang, B.; Kermani, A.; Fillingham, T. Vibrations of Metal Web Joist Timber Floors with Strongbacks. *Proc. Inst. Civ. Eng.—Struct. Build.* **2016**, *169*, 549–562. [CrossRef]
19. *CEN/TS 19103:2021*; Eurocode 5: Design of Timber Structures—Structural Design of Timber-Concrete Composite Structures—Common Rules and Rules for Buildings. European Committee for Standardization: Brussels, Belgium, 2021.
20. MiTek Posi-Joist Brochure—MiTek UK and Ireland. Available online: https://www.mitek.co.uk/wp-content/uploads/sites/23/2018/10/Posi-Joist-Brochure-.pdf (accessed on 27 August 2025).
21. Agris Rogainis Design Methodology Analyse of Timber Concrete Roof with Parallel—Chord Trusses with Steel Lattice. Master's Thesis, Riga Technical University, Riga, Latvia, 2023.